J Electr Eng Technol Vol. 9, No. 4: 1375-1384, 2014
http://dx.doi.org/10.5370/JEET.2014.9.4.1375

ISSN(Print) 1975-0102
ISSN(Online) 2093-7423

Flashover Prediction of Polymeric Insulators Using PD Signal Time-Frequency Analysis and BPA Neural Network Technique

V. Jayaprakash Narayanan*, B. Karthik and S. Chandrasekar†**

Abstract – Flashover of power transmission line insulators is a major threat to the reliable operation of power system. This paper deals with the flashover prediction of polymeric insulators used in power transmission line applications using the novel condition monitoring technique developed by PD signal time-frequency map and neural network technique. Laboratory experiments on polymeric insulators were carried out as per IEC 60507 under AC voltage, at different humidity and contamination levels using NaCl as a contaminant. Partial discharge signals were acquired using advanced ultra wide band detection system. Salient features from the Time-Frequency map and PRPD pattern at different pollution levels were extracted. The flashover prediction of polymeric insulators was automated using artificial neural network (ANN) with back propagation algorithm (BPA). From the results, it can be speculated that PD signal feature extraction along with back propagation classification is a well suited technique to predict flashover of polymeric insulators.

Keywords: Power transmission line, Insulator, Flashover, Partial discharge, Frequency spectrum, Neural networks

1. Introduction

Porcelain and glass have traditionally been widely used as the insulating materials for high voltage power transmission line applications. In recent times, polymeric insulators, made of silicone rubber, have replaced ceramic units due to wide range of reasons such as light weight, easy installation, high mechanical strength to weight ratio, combat to vandalism and superior insulation performance [1, 2]. When these polymeric insulators are installed in coastal areas, the salt and airborne particles are deposited on their surfaces and the pollution builds up gradually. Under dry conditions, these deposits do not decrease the surface insulation strength, whereas in wet weather condition a conductive layer is formed which results in flow of leakage current. The density of leakage current is non-uniform over the surface of the insulator and due to flow of leakage current sufficient heat is developed leading to formation of dry bands in the surface. Formation of dry bands causes redistribution of voltage along the insulator surface giving rise to strong electric field intensity across the dry bands which create electric arcs (or) partial discharges (PD) across the dry bands. This dry band arc will cause erosion and surface degradation of insulating material in polymeric insulators. When the surface resistance is low enough, these dry band arcs will grow along the insulator profile and may eventually cause insulator flashover.

A number of studies have been performed to optimize the maintenance times of outdoor insulators. But it resorts to pollution charts which are widely used and are liable to abnormal seasonal and weather variations. The conventional Equivalent Salt Deposit Density (ESDD) method has been proposed, but it looks both time consuming and difficult to practice [3, 4]. At present, the common technique to predict the flashover is by means of analysis of leakage current. It indicates the surges occurring near the current peaks of dry band arcing phenomena [5-8]. For a given insulator, evolution of leakage waveform depends essentially on the changes occurring at the surface pollution layer and surface wetness of the insulator. Sarathi et al., [9] have proposed the multi resolution decomposition technique as an effective tool to understand time-frequency characteristics of leakage current signals and to identify the surface condition of the insulation.

When these polymeric insulators are installed in outdoor transmission lines, they are also affected by severe weather conditions such as high temperature, large daily and seasonal variations in humidity levels and thermal stress throughout the year. Several studies have been performed to understand the effect of different environmental stresses on the polymeric insulators [10-16]. However, information about the flashover prediction of polymeric insulators considering the thermal stress is rather limited. It is necessary to develop diagnostic techniques for flashover prediction of polymeric insulators considering the effects of both thermal stress and increase in pollution deposits over a time period. The dry band arcs due to wet pollution

† Corresponding Author: Dept. of Electrical and Electronics Engineering, Gnanamani College of Technology, India. (chandrukvt@gmail.com)
* Dept. of Electrical and Electronics Engineering, Gnanamani College of Technology, India. (vanijp2010@gmail.com)
** Dept. of Electrical and Electronics Engineering, Sona College of Technology, India. (karthik_pse@yahoo.co.in)
Received: December 4, 2013; Accepted: February 20, 2014

are a precursor of flash over; hence the partial discharge detection will provide better mechanism to effectively predict the flashover of the outdoor polymeric insulator [17-18]. Considering these facts, this paper implies the effects of conductive pollution on PD activity through laboratory experiments performed on thermal aged polymeric insulator at different pollution levels and at different relative humidity conditions. Typical PD waveforms along with PD patterns have been collected through an innovative PD detection system. Time-frequency map characteristics of PD pulses are observed and important features are extracted from PRPD pattern. Artificial Neural Network, a well defined pattern recognition tool, is used to predict accurately the flashover of polymeric insulators.

2. Experimental Setup

A polymeric insulator of 11 kV rating with leakage distance 300 mm and core diameter 70 mm was used for laboratory experiments. It has wet power frequency withstand voltage of 35 kV, tensile load capacity of 70 kN and operating temperautre range from -100°C to 300°C as per the manufacturers data (Goldstone Infratech Limited, India). Fig. 1 shows the photograph and sketch of the polymeric insulator used in this study.

Fig. 2 reports the schematic diagram of the experimental set up. The test insulator was suspended vertically inside the fog chamber (1.5×1.5×1.5 m). Test voltage was 11 kV rms, 50Hz. Tests were conducted as per IEC 60507 clean fog test procedure. Before tests, the insulator surfaces were cleaned by washing with isopropylic alcohol and rinsing with distilled water, in order to remove any trace of dirt and grease. To reproduce the saline pollution typical of coastal areas, a contamination layer consisting of sodium chloride was sprayed over the surface of the polymeric insulator such that the salinity spread uniformly over the surface [3].

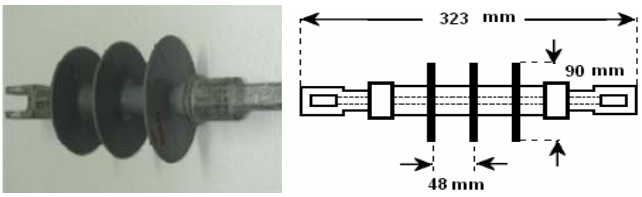

Fig. 1. Photograph and sketch of the 11kV silicone rubber insulator

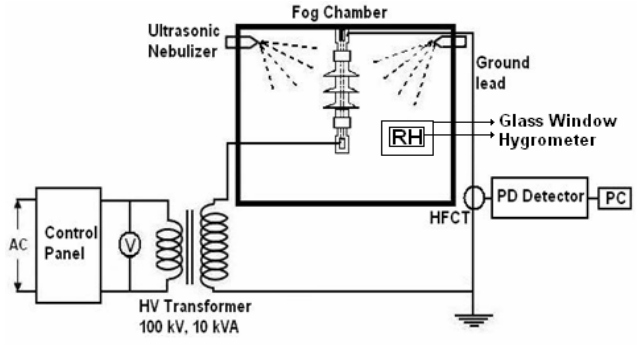

Fig. 2. Schematic diagram of the experimental set up

Concentration of NaCl salt was varied to give Equivalent Salt Deposit Density (ESDD) in mg/cm^2 to 0.06 (lightly polluted), 0.08 (moderately polluted), and 0.12 (heavily polluted). Contaminated insulators were allowed to dry naturally and deionized water droplet of conductivity 5 μS/cm was placed on the surface of contaminated insulator in a discrete area ≈ 2 cm^2. It was sucked into a syringe after 5 minutes and the new conductivity was measured (Horiba Scientific, B-173 compact conductivity meter) and used for ESDD calculation as per ref [3]. Accelerated thermal aging of the polymeric insulator was carried out in the lab by keeping the specimen inside the temperature controlled hot air oven at 150°C for a period of 1440 hr and then samples were taken out for experimental studies. Four Omron ultrasonic nebulizers (NE-U17), which generate particle size of 2-5μm, were used to maintain the required relative humidity inside the fog chamber within a limit of ±5% of required value [18-20]. Relative humidity was measured using the wall-mount Hygrometer (HTC-1) instrument which was kept inside the fog chamber and readings were noted through a glass window fixed on the chamber.

PD signals were picked by connecting a high frequency current transformer (HFCT) around the ground lead. HFCT is a clip on device clamped around the ground lead and it has a 50MHz frequency bandwidth which is sufficient to cover the entire range of PD. Output of the HFCT is connected to the PD detecting instrument, PDBASE II (TechIMP Systems, Italy), which is a large bandwidth system able to sample the complete PD waveforms at a sampling rate of upto 100 MSa/s and bandwidth of 0-50 MHz. Sensitivity of PDBASE II lies in the range of 2 mV/div to 5V/div. It also provides large number of digitized PD pulse waveforms and able to separate them according to the PD waveform shape [21-22]. PD pulses were sent to a remote PC for further processing.

3. Results and Discussion

3.1 PD patterns at different pollution level and relative humidity

In order to understand the difference in PRPD pattern between the clean and polluted surface, initially silicone rubber insulator was tested without applying any pollution at 11kV rms voltage. Insulator specimen was kept inside the fog chamber and tested for both clean dry surface and clean wet surface condition without applying any pollution and the relative humidity level was varied from 50% to 100%. Typical PRPD patterns obtained with the clean surface at 100% RH is shown in Fig. 3. The sine waveform

used in the PRPD pattern is used as a phase reference signal and its amplitude is not given in vertical scale.

It is observed that during both clean tests, there is no significant discharge. Only high frequency noise signal is present in this test. Typical PD pulse and corresponding frequency spectrum obtained at clean surface condition is shown in Fig. 4. From the results, it is observed that PD signal is completely absent and low magnitude noise signals are only present during this measurement. Frequency bandwidth of the noise signal was observed in the range of 20-25 MHz.

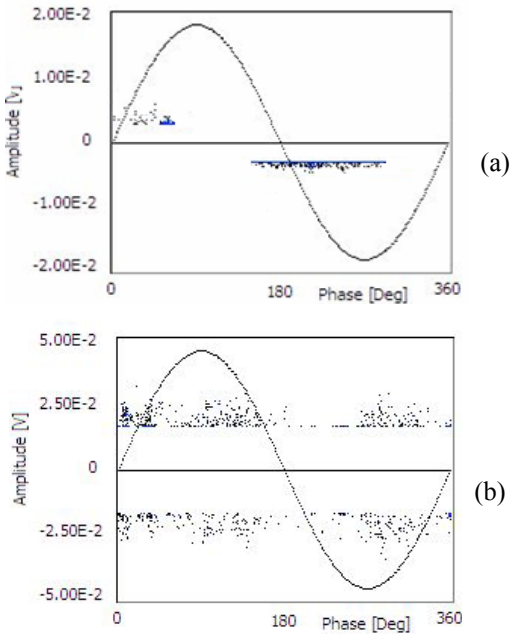

Fig. 3. Typical PRPD pattern of 11 kV polymeric insulator obtained at 100% RH: (a) Clean dry; (b) Clean wet surface

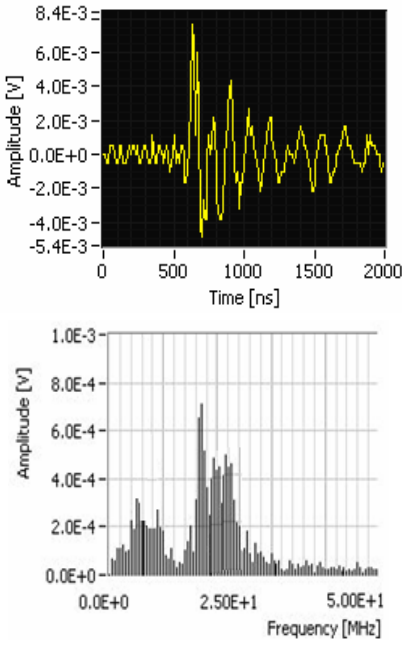

Fig. 4. Typical PD pulse and corresponding frequency spectrum at clean surface condition of insulator

Thermal stress may lead to increased leakage current and which may result in earlier flash over under wet and contaminated conditions. Hence it is necessary to understand the PD characteristics with respect to thermal stress and pollution level on the surface of insulator. Therefore, PD measurement is carried out on thermal aged insulator specimens, by keeping the sample under different pollution level at a constant relative humidity. Typical PRPD pattern obtained at 90% relative humidity is shown in Fig. 5. The contamination level is varied from 0.06 ESDD to 0.12 ESDD in this set of experiments. Occurrence of PD pulses in both positive and negative half cycles is noticed.

By comparing the PRPD patterns of thermal aged specimens, it can be inferred that the magnitude of PD and dispersion of PD amplitude in the pattern increases with respect to increase in pollution level. However, the number of PD pulses at high pollution (0.12 ESDD) is reduced considerably when compared with 0.08 ESDD. This may be due to the formation of long arcs occuring in the surface of the insulator during high pollution, which dries the

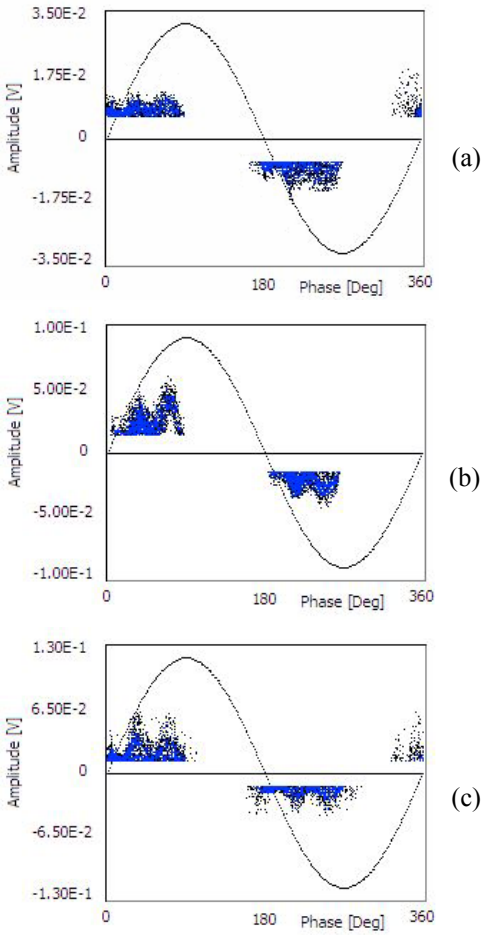

Fig. 5. Typical PRPD pattern of 11 kV thermal aged polymeric insulator obtained at 90% RH: (a) 0.06 ESDD; (b) 0.08 ESDD; (c) 0.12 ESDD

surface quickly and therefore it takes some more time for the initiation of another PD pulse after surface wetting. Photograph of short duration PD pulses and long duration PD pulses of polymeric insulator at 95% relative humidity level are shown in Fig. 6.

Relative humidity plays a major role in the wetting of insulator surface and in the initiaton of partial arcs along the surface of the polluted insulator. Hydrophobic polymers are characterized by high electrical surface resistance which however decreases due to water absorption during ageing and with increasing environmental temperature and contamination build up [23-24]. Hence it is necessary to understand the effect of increase in relative humidity level on the PD activities of the thermal aged polymeric insulator. Therefore, thermal aged polymeric insulators were tested at constant pollution level 0.06 ESDD and the relative humidity inside the fog chamber was varied from 60% to 100%. Fig. 7 shows the typical PRPD pattern obtained at 0.06 ESDD at different relative humidity levels of thermal aged specimens.

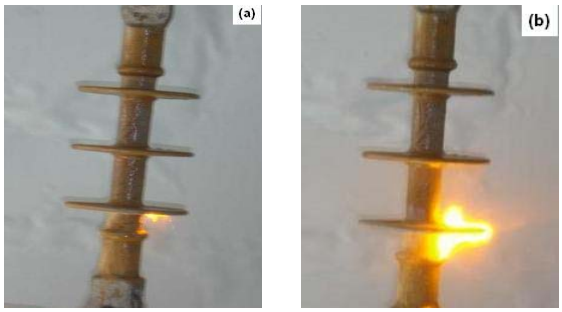

Fig. 6. Photograph of 11 kV polymeric insulator at 95% relative humidity: (a) Short duration PD observed at 0.08 ESDD pollution; (b) Long arc observed at 0.12 ESDD pollution

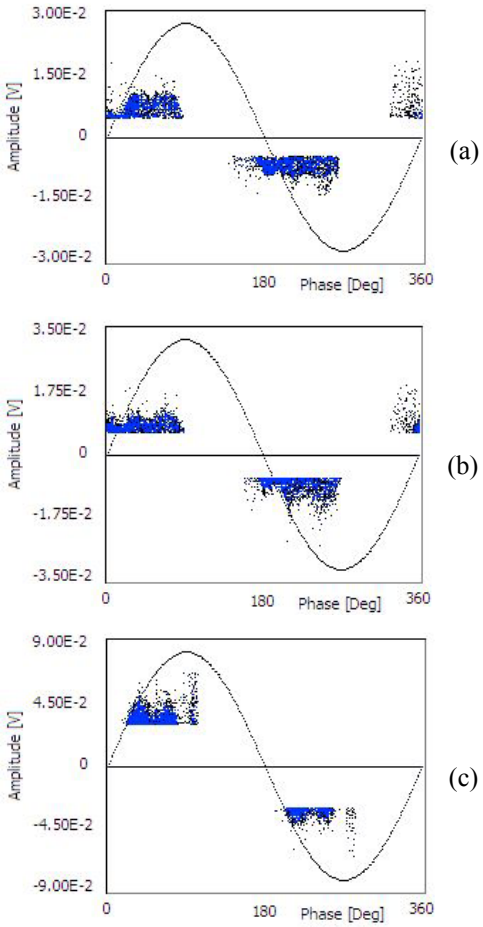

Fig. 7. Typical PRPD pattern of 11 kV thermal aged polymeric insulator obtained at 0.06 ESDD: (a) 60 % RH; (b) 80% RH; (c) 100% RH

From the PRPD patterns, it can be identified that the magnitude of the PD and number of PD pulses increases with increasing relative humidity. Considerable increase in magnitude and dispersion of PD is noticed at all relative humidity levels. This is mainly, because at high relative humidity, the collection of water droplets along the surface of the polymeric insulator is more, causing high leakage current which leads to the heating of surface and causes more dry bands along the surface. Due to increase in electric field strength across the dry bands and surface degradation due to accelerated thermal aging, more number of PD pulse occurs. It is also noticed from the PRPD patterns that with respect to increase in relative humidity level, the dispersion of PD pattern increases, which shows a feature typical of surface discharge phenomena. Occurrence of large number of PD on the surface of thermal aged polymeric insulator causes surface degradation and erosion of the material, which leads to reduction in electrical insulation strength.

3.2 Feature extraction from PRPD pattern

From the PRPD pattern analysis it is observed that PD pulse amplitude increases with increase in pollution level. Hence stochastic features such as PD amplitude and phase variations and its dispersion can be used as an important identification marker for the prediction of flashover of polymeric insulators. In the present work, shape parameter (β) of Weibull PD amplitude distribution, which is a measure of PD amplitude dispersion, is calculated. Also, Mean value of PD amplitude and PD phase is calculated for each measured PRPD pattern.

Figs. 8 (a) and (b) shows the variations in the β and mean phase of polymeric insulator at different pollution levels respectively. It is observed that as the pollution level increases, reduction in β value is noticed which clearly indicates the increase in data dispersion with increase in pollution level. When the value of β reaches below 3, then it indicates heavily polluted surface conditionand possibility of flashover. Mean phase value of PRPD pattern increases considerably with respect to increase in pollution level. If it goes above 45 degrees then it indicates highly polluted surface condition, which indicates the possibility

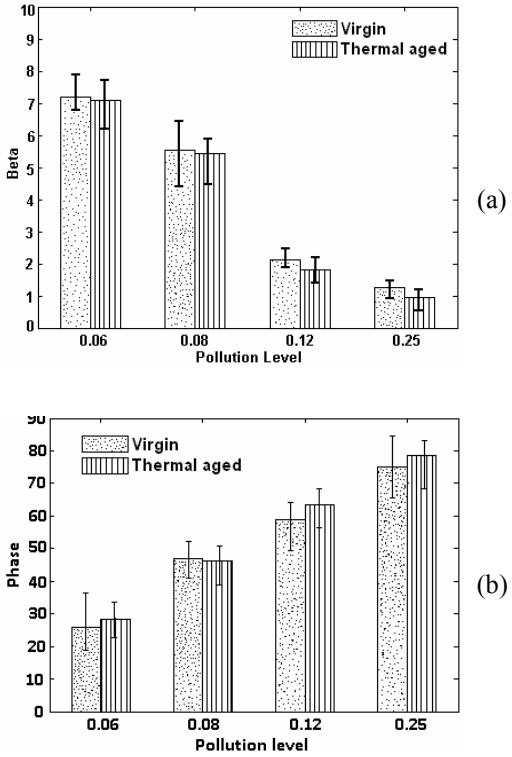

Fig. 8. Variations in the (a) β and (b) mean phase of virgin and thermal aged insulators at different pollution levels

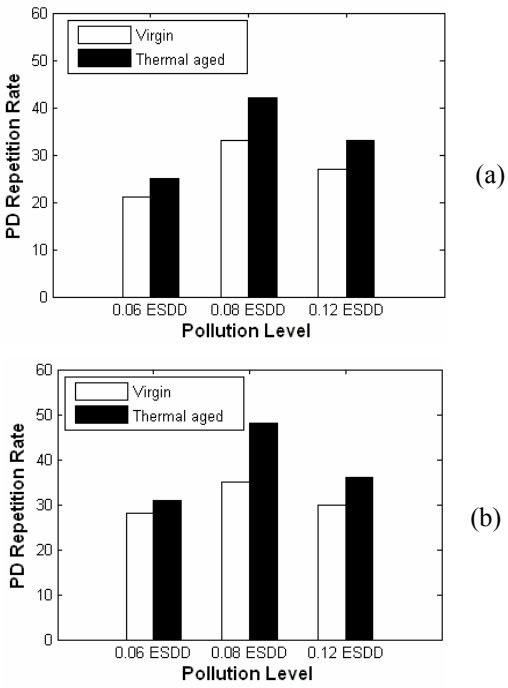

Fig. 9. PD repetition rate of virgin and thermal aged polymeric insulator at: (a) 80% RH and (b) 100 % RH

for flashover.

3.3 Feature extraction from repetition rate analysis of PD pulses

Repetition rate of the PD pulses (pulses/sec) is a good indicator of flashover on the surface of the insulator and it is also indirectly a measure of surface degradation of the polymeric insulators. In the case of outdoor polymeric insulators, the PD appear in pulse bursts and their repetition rate is irregular. Fig. 9 shows the plot between repetition rate and pollution level of polymeric insulators at different relative humidity conditions. In general, the repetition rate of the PD pulses increases with increase in pollution level and relative humidity level. Once the partial discharge inception starts, the repetition rate rises gradually with respect to increase in pollution and when the pollution level reaches the maximum to 0.12 ESDD, it shows a reduction in repetition rate. Similar trend is obtained for both virgin and thermal aged specimens; however the magnitude of repetition rate is considerably higher for thermal aged specimens when compared with virgin specimens. Rate of rise of repetition rate is higher for 100 % RH level when compared with 80 % RH level. The reason for sudden decrease in repetition rate at high pollution may be due to the formation of long partial arcs along the surface which heats the surface and causes a time lag for the formation of next partial arc. This clearly shows that PD repetition rate can be used as additional information to predict the flashover.

3.4 Time and frequency domain analysis of PD signals

Understanding the time and frequency domain characteristics of PD signal is important in order to extract important features and develop a better diagnostic system for the flashover prediction of polymeric insulators. In the present work, during the experimental studies, individual PD pulses were also captured simultaneously at different pollution conditions and stored in PC for frequency domain analysis. Typical PD pulses and its corresponding frequency spectrum of thermal aged insulators obtained at different surface pollution conditions are shown in Fig. 10. Short duration discharges (Figs. 10 (a) and (b)) are mostly observed at lightly polluted conditions, whereas long duration discharges are observed at heavily polluted conditions (Fig. 10(c)). Time length and rise time of PD pulses increases considerably with respect to increase in pollution level. At lightly polluted conditions (0.06 ESDD), the high frequency content (15-25 MHz) is also noticed in the frequency spectrum of the PD signal. With respect to increase in pollution level from 0.06 ESDD to 0.12 ESDD, the magnitude of high frequency content (15-25 MHz) significantly reduces and the dominant frequency content shifts towards 5-10 MHz. Energy content of the PD signal increases at long arcs and this will increase the surface

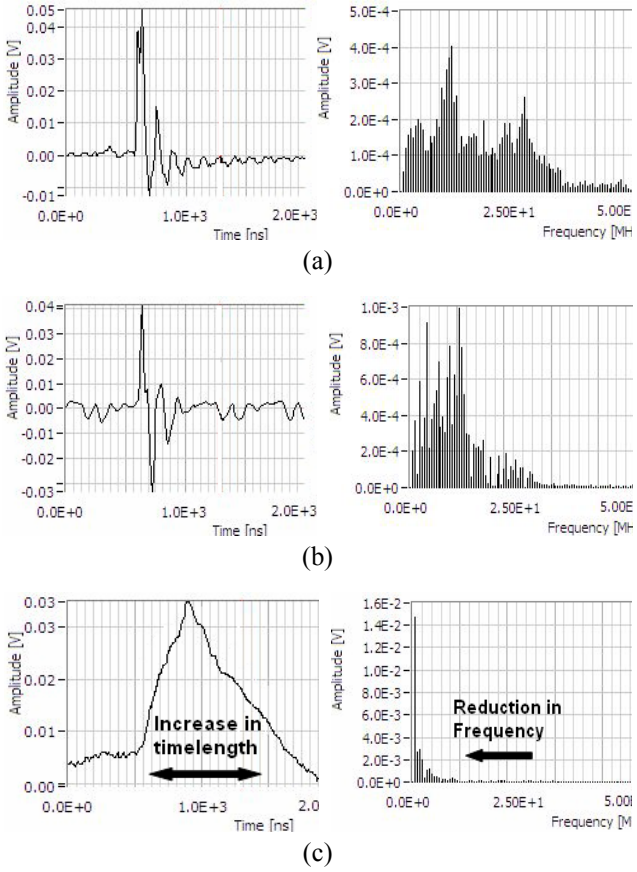

Fig. 10. PD pulse and frequency spectrum of thermal aged polymeric insulator obtained at 90 % RH: (a) 0.06 ESDD; (b) 0.08 ESDD; (c) 0.12 ESDD

local temperature of the thermal aged specimens, which will lead to faster erosion and degradation of the polymeric material.

3.5 Feature extraction from equivalent timelength-equivalent bandwidth map

In the case of on-line outdoor PD measurements on transmission tower insulators, the presence of significant noise and/or pulses coming from various PD sources active at the same time will make the diagnosis of flashover of insulators extremely difficult even for skilled operators. Accurate diagnosis based on PD analysis depends on effective noise/disturbance rejection and on the collection of large amount information on PD signals. Hence it is necessary to classify the large collection of PD signals based on the equivalent timelength and equivalent bandwidth, i.e. the two real numbers used to localize the PD signal in time/frequency plane [15]. Partial discharge detection system finds the equivalent time length and equivalent bandwidth of PD pulse and clusters the data into different groups in the time/frequency map. In particular, let s(t) be the time domain representation of PD pulse, then equivalent time length and equivalent bandwidth are

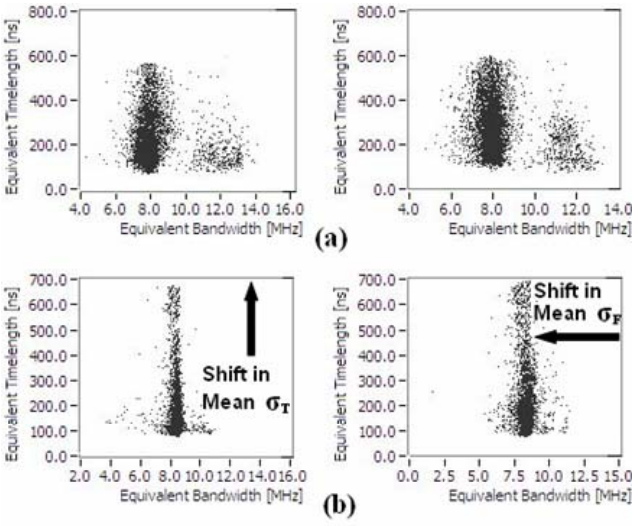

Fig. 11. Typical equivalent timelength-bandwidth plot of virgin (left) and thermal aged (right) specimen at 100 % RH: (a) 0.06 ESDD; (b) 0.12 ESDD

obtained using [25-26],

$$\sigma_T = \sqrt{\int_0^T (t-t_0)^2 \tilde{s}(t)^2 dt} \quad (1)$$

$$\sigma_F = \sqrt{\int_0^\infty f^2 \left|\tilde{S}(f)\right|^2 df} \quad (2)$$

where f is the frequency, $\tilde{S}(f)$ is the Fourier transform of the normalized pulse $\tilde{s}(t)$.

Fig. 11 shows the typical equivalent timelength-equivalent bandwidth map of PRPD pattern obtained at 100 % RH of virgin and thermal aged specimen at different pollution level. In this time/frequency plane, equivalent time length is represented in ns and equivalent bandwidth is represented in MHz. PD pulses are reduced to two real numbers by (1) and (2) and represented as a dot in the time/frequency plane. Since the PD measurements were carried out above noise level in the laboratory, presence of high frequency noise signals above 20 MHz is completely absent in this represenation. It is observed that PD signals lies in the frequency band of 6 MHz to 12 MHz. However, most of the PD signals lies in the frequency band of 7-9 MHz. It is also noticed that PD signals lying in the 7-9 MHz bandwidth has varying timelength from 100 ns to 700 ns. Increase in equivalent timelength above 600 ns of the PD signal clearly related with long arcs obtained at high pollution (0.12 ESDD).

In the case of thermal aged specimens at high pollutions (Fig. 11(b)), the presence of long arcs above 600 ns is higher when compared with virgin specimens. With respect to increase in pollution, it is also observed that the frequency content in 10-13 MHz range reduces. It is noticed that there is an increase in mean equivalent time length and reduction in mean equivalent bandwidth with respect to increase in pollution level of both virgin and

thermal aged specimen. Hence, mean equivalent time length and mean equivalent bandwidth are extracted as an important feature from this time-frequency plane. This time/frequency plane analysis clearly indicates the increase in long arcs due to pollution, which will lead to flashover on the surface of the insulator.

3.6 Prediction of surface pollution severity using artificial neural network

In order to automate the prediction of flashover of insulator, Artificial Neural Network (ANN) was used. ANN is a highly parallel, adaptive learning system that can learn a task by generalizing from case studies of the tasks. In the present work, the Multilayer Feed Forward network with back propagation learning algorithm has been used because of its good generalization capability. The details of the neural network parameters are shown in Table 1.

In the present work, multilayer feedforward neural network with an input layer, one hidden layer and an output layer is used. Shape parameter (β) of PD amplitude distribution, mean PD amplitude, mean PD phase, mean equivalent time length, mean equivalent bandwidth and PD repetition rate are given as an input to the neural network. The 4 output neurons were used to classify as no discharge, short duration discharge, long duration discharge and flashover. The training phase consists of the iterative presentation of the six inputs with the estimated output, the adjustment of the weights and biases depending on the resultant error. The convergence is reached when the error between the measured and the desired output is less than convergence criteria. In this network, error is back propagated and weights and biases are conveniently readjusted in order to minimize the Mean Square Error (MSE), which is the average of sum of the errors for all set of inputs and corresponding outputs, which is calculated as,

$$MSE = \frac{1}{m}\sum_{k}^{m}\left(S_k - Y_k\right)^2 \quad (3)$$

where S_k and Y_k are respectively the desired and measured output for the k^{th} input set and m is the total number of input sets.

There are several factors which influence the performance of the neural network and therefore optimization of neural network parameters is important for the development of efficient diagnostic system. Initially, MSE was evaluated at different number of hidden layer neurons as shown in Fig. 12. It indicates that the MSE value obtained with 14 hidden layer neurons is the minimum. As the number of hidden layer neurons increases, the neural network takes more time to learn.

Fig. 13 shows the performance of the network during training with 14 hidden layer neurons at different iteration numbers. It clearly indicates that the present network

Table 1. Neural network specifications

No. of inputs	6
No. of neurons in hidden layer	14
No. of neurons in output layer	4
Learning rate (η)	0.01
No. of iterations	3500
No. of training sets	200
No. of test input sets	100
Convergence criteria	0.01

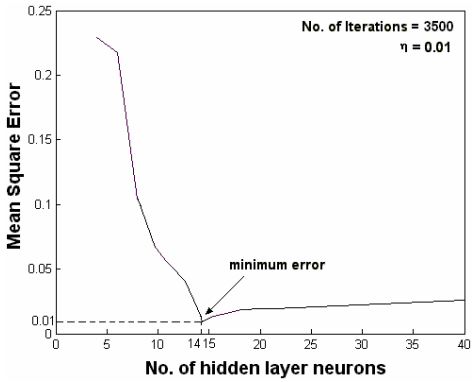

Fig. 12. Evaluation of the mean square error of the neural network at different no. of hidden layer neurons

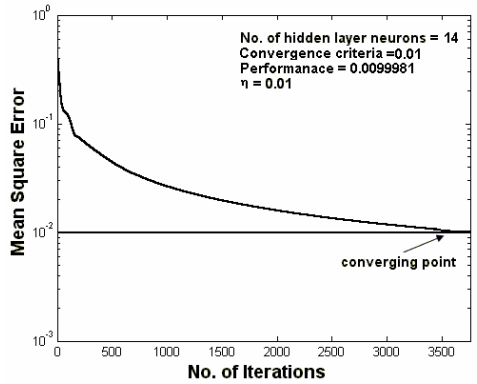

Fig. 13. Evaluation of mean square error of the neural network at different no. of iterations

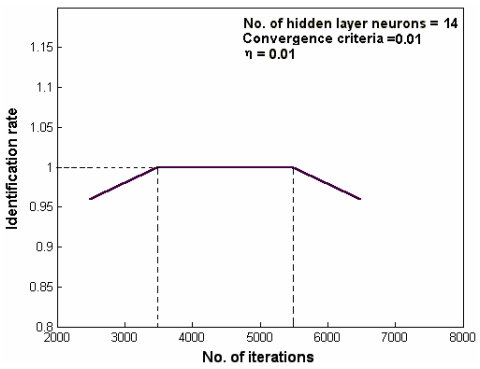

Fig. 14. Evaluation of identification rate at different no. of iterations with optimized value neural network parameters.

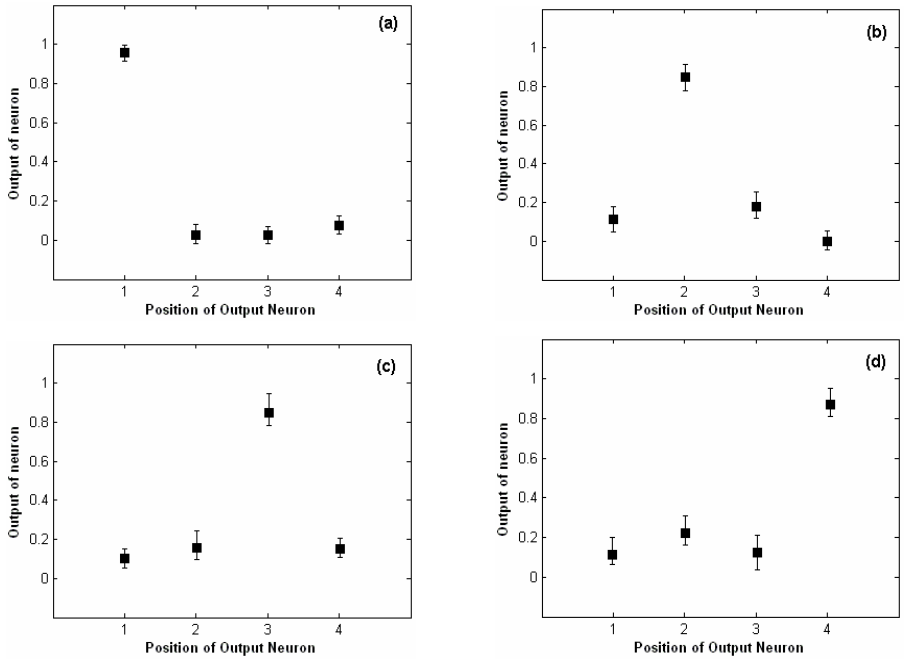

Fig. 15. Output of neurons in the output layer of the neural network: (a) No discharge; (b) Short duration discharge; (c) Long duration discharge; (d) Flashover

Table 2. Identification rates at different η

Learning Rate η	0.01	0.1	0.2	0.3
Identification Rate (%)	100	100	98	96

reaches the convergence criteria near 3500 iterations. Fig. 14 shows the identification rate of the network at different no. of iterations at optimized value of hidden layer neurons and learning rate. It clearly indicates that 100 % success rate is achieved from 3500 to 5000 no. of iterations and therefore 3500 iterations is sufficient for the successful training of the optimized neural network. In the back propagation network, the speed and accuracy of the learning process i.e. the process of updating the weights, depends on learning rate η. Identification rates of back-propagation network with different learning rates are shown in Table 2. In the neural networks, high values of learning rate results in fast convergence, but the network accuracy and the identification rate reduces. The optimum value of learning rate is found to be 0.01.

Fig. 15 shows the identification results of the output of the neuron in the output layer of the optimized neural network (no. of hidden layer neurons = 14, η = 0.01, convergence criteria=0.01, no. of iterations=3500). For example, if the input pattern corresponds to "no discharge" case, then the four neurons in output layer are trained for a pattern (1 0 0 0). Therefore, when a "no discharge" case which is not trained in the NN is given as an input, it is expected that the output pattern will be closer to (1 0 0 0). Fig. 16 (a) shows the output of the neurons in output layer for "no discharge" input. It is clear that output of 1st neuron is closer to 1 and all other neurons mostly give an output below 0.2. Similarly, Figs. 16 ((b), (c) and (d)) shows the output of neurons at other discharge conditions. In this work, it is observed that the recognition rate in most of the case is above 0.75. This indicates that the trained neural network can predict the flashover of the polymeric insulator accurately and continuously in the electrical power network.

The reported partial discharge characteristics such as PRPD pattern, PD pulse-frequency spectrum, repetition rate and equivalent time length-equivalent bandwidth analysis show that flashover of polymeric insulators can be assessed by looking at the evolution of PD- related quantities in the course of time. When compared with PD test results of virgin insulators under similar experimental conditions, it is noticed that thermal aged silicone rubber insulator shows increased PD activity, which will certainly lead to surface erosion and degradation. Artificial neural network approach with back propagation training algorithm effectively predicts the flashover and pollution severity of polymeric insulators.

4. Conclusion

Laboratory measurement and analysis of partial discharge pattern and PD pulses of silicone rubber insulators has been presented in this paper. Laboratory tests are performed at different relative humidity and pollution levels as per IEC 60507 test procedure. It is shown that variations in time and frequency domain characteristics of PD pulses are closely related to the surface pollution

condition of the polymeric insulator. When compared with PD test results of virgin insulators, it is noticed that thermal aged silicone rubber insulator shows increased PD activity, which will certainly lead to surface erosion and degradation. Equivalent timelength-equivalent bandwidth plane clearly shows the increase in pollution level on the surface of insulator and it can be used as a diagnostic tool to predict the flashover of insulator. Extracted features from PRPD pattern and time-frequency map are used as an identification marker of flashover of polymeric insulators. Artificial neural network approach with back propagation training algorithm effectively predicts the flashover of polymeric insulators. These lab results on thermal aged polymeric insulator shows that, when these insulators are used in tropical regions, they are exposed to large thermal and ambient stress variations for the entire life span which will accelerate the surface degradation of the material under severe pollution conditions, which may lead to reduced insulation strength and possibility of surface flashover.

Acknowledgements

Author(S.C) would like to sincerely thank Tech IMP, Italy for their support in the partial discharge measurements.

References

[1] J.S.T. Looms, *Insulators for high voltages*, IEE series, 1990.

[2] R.S. Gorur, E.A. Cherney and J.T. Burnham, *Outdoor Insulators*, Ravi S. Gorur Inc Phoenix, Arizona 85044, USA, 1999.

[3] IEC 60507, *Artificial Pollution tests on high voltage insulators to be used on AC systems*, 1991.

[4] G.R.Montoya and J.I.Montoya, "Correlation among ESDD, NSDD and leakage current in distribution insulators", *in IEE Proc. Generation, Transmission and Distributions*, vol.151, pp. 334-340, 2004.

[5] F. Kawa, M. J. Chavez, T. Orbeck and C. Lumb, "Practical PCADA system for measurements of leakage current pulses on polymer insulators under wet contaminated conditions", *IEEE Electr. Insul. Mag*., vol.8, no.2, pp.5-13, 1992.

[6] Hadi Hosseini Kordkheili, Hassan Abravesh, Mehdi Tabasi, Marzieh Dakhem and Mohammad Mehdi Abravesh, "Determining the Probability of Flashover Occurrence in Composite Insulators by Using Leakage Current Harmonic Components", *IEEE Trans. on Dielectrics and Electr. Insul.*, vol.17, no.2, pp.502-512, April 2010.

[7] Suwarno, "Leakage Current Waveforms of Outdoor Polymeric Insulators and Possibility of Application for Diagnostics of Insulator Conditions", *Journal of Electrical Engineering & Technology*, vol.1, no.1, pp. 114-119, 2006.

[8] C. Muniraj, K.Krishnamoorthi and S.Chandrasekar, "Investigation on Flashover Development Mechanism of Polymeric Insulators by Time Frequency Analysis", *Journal of Electrical Engineering & Technology*, vol.8, no.6, pp.1503-1511, 2013.

[9] R. Sarathi, S. Chandrasekar and N. Yoshimura, "Investigations into the Surface Condition of the Silicone Rubber Insulation Material using Multi-resolution Signal Decomposition", *IEEE Trans. Power Delivery*, vol.21, pp.243-252, 2006.

[10] Zeinab Farhadinejad, Morteza Ehsani, Iman Ahmadi-Joneidi, Amir Abass Shayegani and Hosein Mohseni, "Effects of UVc Radiation on Thermal, Electrical and Morphological behavior of Silicone Rubber Insulators", *IEEE Trans. Dielectrics and Electr. Insul.*, vol.19, no.5, pp.1740-1749, October 2012.

[11] B.Venkatesulu and M. Joy Thomas, "Long –term Accelerated Weathering of Outdoor Silicone Rubber Insulators", *IEEE Trans. Dielectrics and Electr. Insul.*, vol.18, no.2, pp.418-424, April 2011.

[12] Mitra Khiabani Moghadam, Jalil Morshedian, Morteza Ehsani and Mozhgan Bahrami, "Lifetime Prediction of HV Silicone Rubber Insulators based on Mechanical Tests after Thermal Ageing", *IEEE Trans. Dielectrics and Electr. Insul.*, vol.20, no.3, pp.711-716, June 2013.

[13] M.A.R.M.Fernando and S.M.Gubanski, "Ageing of Silicone Rubber Insulators in Coastal and Inland Tropical Environment", *IEEE Trans. Dielectrics and Electr. Insul.*, vol.17, no.2, pp.326-333, April 2010.

[14] Iman Ahmadi-Joneidi, Alireza Majzoobi, Amir Abbas Shayegani-Akmal, Hossein Mohseni and Jouya Jadidian, "Aging Evaluation of Silicone Rubber Insulators Using Leakage Current and Flashover Voltage Analysis", *IEEE Trans. Dielectrics and Electr. Insul.*, vol. 20, no. 1, pp. 212-220, Feb 2013.

[15] R.S. Gorur and H.M. Schneider, "Surface resistance measurements on non-ceramic insulators", *IEEE Trans. Power Delivery*, vol. 16, pp. 801-805, 2001.

[16] W. Que, E.P. Casale and S.A. Sebo, "Voltage-Current phase angle measurements during aging tests of polymer insulators", *in Proc. IEEE CEDIP*, 2002, pp 367-370.

[17] A. Cavallini, S. Chandrasekar and G. C. Montanari, "Inferring Ceramic Insulator Pollution by an innovative Approach Resorting to PD Detection", *IEEE Trans. Dielectrics and Electr. Insul.*, vol. 14, no. 1, pp. 23-29, 2007.

[18] S.Chandrasekar, C.Kalaivanan, G.C.Montanari and A.Cavallini, "Partial Discharge Detection as a tool to infer Pollution Severity of Polymeric Insulators", *IEEE Trans. Dielectrics and Electr. Insul.*, vol 17, pp.181-188, 2010.

[19] S. Venkataraman and R.S. Gorur, "Prediction of flashover voltage of non-ceramic insulators under contaminated conditions", *IEEE Trans. Dielectrics and Electr. Insul.*, vol. 13, no.4, pp. 862-869, 2006.

[20] Shihua Zhao, Xingliang Jiang, Zhijing Zhang, Jianlin Hu, And Lichun Shu, "Flashover voltage prediction of composite insulators based on The characteristics of leakage current", *IEEE Trans. Power Delivery*, vol. 28, no. 3, pp. 1699-1708, 2013.

[21] A. Cavallini, A. Contin, G.C. Montanari and F. Puletti, "Advanced PD inference in on-field measurements. Part I. Noise rejection", *IEEE Trans. Dielectrics and Electr. Insul.*, vol. 10, pp. 216-224, 2003.

[22] A.Cavallini, M.Conti, A.Contin and G.C.Montanari, "Advanced PD Inference in On-Field Measurements. Part. 2: Identification of Defects in Solid insulation Systems", *IEEE Trans. Dielectrics and Electr. Insul.,* Vol. 10, pp. 528-538, 2003.

[23] S. H. Kim, E. A. Cherney and R. Hackam, "Hydrophobic behavior of Insulators Coated with RTV Silicone Rubber", *IEEE Trans. Electr. Insul.,* Vol 27, pp. 610-622, 1992.

[24] S. Kumagai, N. Yoshimura and S. Nishimura, "Electrical and Environmental aging of Silicone rubber used in outdoor insulation", *IEEE Trans. Dielectrics and Electr. Insul.*, vol. 6, pp. 632-650, 1999.

[25] A.Contin, A.Cavallini, G.C.Montanari, G.Pasini and F.Puletti, "Digital Detection and Fuzzy Classification of Partial Discharge Signals", *IEEE Trans. Dielectrics and Electr. Insul.*, vol. 9, pp. 335-348, 2002.

[26] A.Cavallini, G.C.Montanari, F.Puletti and A.Contin, "A New Methodology for the Identification of PD in Electrical Apparatus: Properties and Applications", *IEEE Trans. Dielectrics and Electr. Insul.,* vol. 12, no. 2, pp. 203-215, 2005.

V. Jayaprakash narayanan was born in India, in 1973. He received the B.E degree in Electrical and Electronics Engineering from Government college of Engineering in Salem, Tamilnadu and M.E degree in power systems engineering from Anna University, India and presently he is pursuing Ph.D in Anna University, Chennai. Currently he is working as Assistant professor at Gnanamani college of Technology in the department of Electrical and Electronics Engineering. His research interests are insulation in power apparatus, digital signal processing and neural networks technique.

B. Karthik was born in India, in 1982. He obtained his B.E degree in Electrical and Electronics Engineering from Annamalai University, Tamil nadu, India in 2003 and ME Degree in power systems engineering from Sona college of technology, Anna University, India in 2006 and Ph.D degree from Anna University, Chennai in India in 2013. Presently, he is working as Assistant Professor at Sona College of Technology in the Department of Electrical and Electronics Engineering. His research interests are high voltage insulation systems, power flow control in transmission line, FACTS device for power quality and new technologies to enhance power system control and monitoring.

S. Chandrasekar was born in India, in 1975. He received the B.E. degree in Electrical and Electronics Engineering from Thiagarajar college of Engineering, Madurai in 1996 and M.E degree in Power Systems Engineering from Coimbatore Institute of Technology, Coimbatore in India in 2001 and the Ph.D degree from Indian Institute of Technology Madras, India in 2005. He was a postdoctoral research fellow at the University of Bologna, Italy from 2005 to 2006. Currently, he is working as a Professor and Principal at Gnanamani College of Technology. He is the head of GnanEXPERT (Electric Power Engineering Research and Testing Centre). His research interests include condition monitoring of power apparatus and systems, insulation engineering, signal processing and artificial intelligence techniques applications in electric power engineering.